9th AIAA/ASME Joint Thermophysics and Heat Transfer Conference
5 - 8 June 2006, San Francisco, California

AIAA 2006-3602

Hybrid Particle-Continuum Simulations of Non-Equilibrium Hypersonic Blunt Body Flow Fields

Thomas E. Schwartzentruber*, Leonardo C. Scalabrin† and Iain D. Boyd‡
Department of Aerospace Engineering, University of Michigan, Ann Arbor, MI 48109

A modular particle-continuum (MPC) numerical method is presented which solves the Navier-Stokes (NS) equations in regions of near-equilibrium and uses the direct simulation Monte Carlo (DSMC) method where the flow is in non-equilibrium. The MPC method is designed specifically for steady-state, hypersonic, non-equilibrium flows and couples existing, state-of-the-art DSMC and NS solvers into a single modular code. The MPC method is tested for 2D flow of N_2 at various Mach numbers over a cylinder where the global Knudsen number is 0.01. For these conditions, NS simulations significantly over-predict the local shear-stress, and also over-predict the peak heating rate by 5-10% when compared with full DSMC simulations. DSMC also predicts faster wake closure and 10-15% higher temperatures in the immediate wake region. The MPC code is able to accurately reproduce DSMC flow field results, local velocity distributions, and surface properties up to 2.8 times faster than full DSMC simulations. The computational time saved by the MPC method is directly proportional to the fraction of the flow field which is in near-equilibrium. It is found that particle simulation of the shock interior is not necessary for accurate prediction of surface properties, however particle simulation of the boundary layer and near-wake region is.

I. Introduction

NUMERICAL simulation of a spacecraft's hypersonic entry into a planet's atmosphere is a vital technology required for the exploration of the solar system. Reproducing such high energy, low density flows in wind tunnel experiments is very expensive and for many flows is currently not even possible. Such spacecraft generally transition from high-speed, rarefied conditions to lower speed, continuum conditions. Furthermore, at intermediate altitudes, within a mostly continuum flow, there may be local regions of rarefied (or *non-equilibrium*) flow generated by both the rapid expansion in the wake of the spacecraft as well as by strong gradients in shock waves and boundary layers. Ultimately, it is the flow conditions inside the wake and boundary layer that determine the drag and heat transferred to the spacecraft surface. Thus it is important that these regions be simulated accurately using an appropriate physical model.

A. Motivation

When continuum conditions are present, the Navier-Stokes (NS) equations may be solved using algorithms from Computational Fluid Dynamics (CFD). Although very efficient, solution of the NS equations in non-equilibrium regions can lead to significant error in flow field and surface properties. The most popular numerical method for simulating high-speed, non-equilibrium flow is the direct simulation Monte Carlo (DSMC) method developed by Bird.[1] The DSMC method is accurate in all flow regimes but requires the computational cell size and time-step to be on the order of the local mean-free-path and mean-free-time respectively. Thus DSMC becomes very computationally expensive as the flow nears continuum conditions. However, it is precisely under these continuum conditions where the NS equations can be solved efficiently without the same restriction on cell size. A review of numerical simulations using both methods and their agreement with various hypersonic, blunt body experiments is presented in Ref. 2. One conclusion of this review article is that while the NS results generally match DSMC and experimental data in the fore-body flow, they deviate significantly from DSMC and experiment in the near-wake for both surface and flow features. In

*Graduate Student, Student Member AIAA. Email: schwartt@umich.edu.
†Graduate Student, Student Member AIAA. Email: lscalabr@umich.edu.
‡Professor, Associate Fellow AIAA. Email: iainboyd@umich.edu.

order to obtain more accurate results in the near-wake region without resorting to a full DSMC simulation, "zonally decoupled" DSMC-NS simulations[3] have been performed. Here, the fore-body flow is solved separately using a NS solver and the exit-plane solution is specified as the inflow condition to a decoupled DSMC simulation of the entire wake region. Results of the zonally decoupled simulations agree well with full DSMC solutions in the wake region, while requiring only half of the computational resources (CPU time and memory).[3] Comparison between zonally decoupled, full DSMC, and full NS simulations also emphasizes the importance of modelling rarefied effects such as thermal non-equilibrium and slip flow in order to predict surface properties and wake closure. Using a similar decoupled approach, the flow about the Mars Sample Return Orbiter was simulated at both flight conditions[4] and for a wind tunnel experiment.[5] The interface between NS and DSMC regions was taken as a plane cutting through the aeroshell lip. Although this practical approach was much more efficient than a full DSMC simulation, in one simulation, 20 million cells were used in the wake region. This required 200 million particles taking 18 Gbytes of core memory and it is reported that regions of the flow may still be under-resolved.[5] Thus, there is significant efficiency to be gained if the DSMC method is restricted only to that portion of the flow field where large non-equilibrium effects are felt.

B. Coupled hybrid methods

Various researchers have proposed hybrid numerical methods which adaptively re-position the DSMC-NS interface during the simulation and couple the two solvers by transferring information across this interface. Reference 6 presents a discussion of the major considerations involved as well as a summary of published work on such coupled schemes. The most problematic aspect is the transfer of information from particle to continuum cells and the inherent statistical scatter in that information. Some researchers determine the average flux of mass, momentum, and energy carried by DSMC particles as they cross the interface and impose this as the macroscopic flux into the neighboring NS cell. Such "flux-based" coupling was used by Hash and Hassan to couple the DSMC method with a NS solver for simulations of Couette flow[7] and hypersonic flow over a blunted cone.[8] More recently, Wijesinghe *et al* also used flux-based coupling to embed a DSMC solver in the finest level of an adaptive mesh and algorithmic refinement (AMAR) scheme for the Euler equations.[9] Although flux-based coupling may seem a natural way to couple particle and continuum solvers, the statistical scatter inherent in determining average flux quantities in a DSMC simulation is very high. In regions where the interface is aligned parallel with the flow direction, the vast majority of particles move along the interface compared to the relatively few which cross the interface. As a result of this small sample size for DSMC flux quantities crossing such an interface, the statistical scatter becomes far too large to impose on the NS domain.[10] An alternate method of information transfer between DSMC and NS domains is to use "state-based" coupling. Here, particles inside a DSMC cell near the interface are averaged to obtain a macroscopic state such as bulk velocity, temperature, and density. The statistical scatter involved in obtaining state quantities is much smaller than that associated with obtaining flux quantities.[6] The averaged macroscopic state is then used as a standard boundary condition for the NS domain. Roveda *et al* used state-based coupling to combine the DSMC method with an Euler solver to simulate moving 1D shock waves[11] and 2D unsteady slit flow.[12] Although use of state-based coupling involved less statistical scatter, their method was time accurate and particle information had to be averaged at each time-step. This significantly constrained the number of samples used for the average. In order to deal with this, the authors employed a novel algorithm to effectively "clone" particles near the interface in order to reduce the statistical scatter transferred to the continuum domain. Wang and Boyd used the Information Preservation (IP) scheme[13] which, in addition to microscopic information, also preserves macroscopic information for each DSMC simulation particle in order to reduce the statistical scatter. Although successful for certain 2D flows,[14] when applied to 1D normal shock waves, it was found that the IP scheme produced an incorrect post-shock state and a shock wave that was too thin. A new formulation for the IP energy flux[15] was able to remedy these problems somewhat, however, at large computational expense.

The hybrid particle-continuum method used in this article is designed specifically for steady-state, hypersonic flows. A similar algorithm has been successfully tested for 1D normal shock waves[16] and is here extended and modified for 2D flows. To begin with, the high velocities associated with hypersonic flow greatly reduce the influence of statistical scatter, making DSMC an efficient method in this regime. By further restricting the algorithm to steady-state flows, temporal averaging combined with state-based coupling is able to effectively manage statistical scatter. Focusing on steady-state flows also allows use of an implicit NS solver, enabling time-scale decoupling which results in significant computational savings. Finally, state-based coupling allows for information transfer to be handled by the standard boundary procedures used by both DSMC and NS solvers. Taking advantage of these ideas, the hybrid DSMC-NS method used in this article is implemented in a novel modular way. The algorithm combines *existing* state-of-the-art DSMC and NS solvers (virtually un-modified) into one modular particle-continuum (MPC) numerical method. This article will briefly outline the details of the MPC method and then use it to analyze non-equilibrium

effects in simple hypersonic blunt body flows from a unique perspective.

II. Modular Particle-Continuum Numerical Method

A. NS and DSMC Solvers

The MPC code described in this article divides the flow field into particle regions where the DSMC method is used and continuum regions where the NS equations are solved. Existing, state-of-the-art codes are used which have been extensively validated. Complete details about each code can be found in the references.

The DSMC portion is simulated using MONACO,[17] a general, cell-based implementation of the DSMC method. The variable hard sphere (VHS) collision model is employed which results in the following macroscopic viscosity model:[1]

$$\mu = \mu_{ref}\left(\frac{T}{T_{ref}}\right)^{\omega} \quad , \qquad \mu_{ref} = \frac{15\sqrt{\pi m k T_{ref}}}{2\pi d_{ref}^2(5-2\omega)(7-2\omega)} \tag{1}$$

All numerical results presented in this article are for diatomic nitrogen (N_2) with a reference diameter of $d_{ref} = 4.17\times10^{-10}$ m at $T_{ref} = 273$ K. The power law exponent, ω, is set equal to 0.75, m is the mass of an N_2 molecule, and k is the Boltzmann constant. MONACO employs the variable rotational energy exchange probability model of Boyd[18] where the reference temperature for rotational energy exchange is specified as 91.5 K and the maximum rotational collision number as 18.1. Energy transfer to vibrational modes is not considered.

The continuum portion is simulated using the LeMANS code.[19] For the results presented in this article, it is assumed that rotational and translational energy modes can be described by a single temperature T. The vibrational energy mode is not considered. The resulting governing equations are the two-dimensional, laminar, compressible, Navier-Stokes equations. The viscosity is modelled using Eq. 1 in order to match exactly the viscosity model used in DSMC. This is important not only at DSMC-NS interfaces (for information transfer) but also whenever comparing DSMC and NS flow field results and surface properties. LeMANS solves this set of equations using a finite-volume formulation. The inviscid fluxes between the mesh volumes are discretized using a modified form of the Steger-Warming Flux Vector Splitting[20] which is less dissipative and adequate to calculate boundary layers. The scheme switches back to the original form of Steger-Warming near shock waves. The viscous terms are calculated using the values of properties at the cell centers and at the nodes. Wall boundaries employ a no-slip condition and inflow and outflow boundaries are treated as supersonic. Finally, the time integration is performed using a point-implicit method. Specific details of the numerical method are contained in Ref. 19.

Hypersonic flow about a 2D cylinder at Mach 3, 6, and 12, is simulated in cases denoted as **M3**, **M6**, and **M12** respectively. The free-stream gas is N_2 with a number density $n = 1.61\times10^{21}$ $1/m^3$ and $T = 217.45$ K. This corresponds to an altitude of 70 km, where $p = 4.83$ Pa and $\rho = 7.48\times10^{-5}$ kg/m^3. The diameter of the cylinder is 8.0 cm resulting in a global Knudsen number of 0.01. Only the free-stream velocities differ for each case and are set to achieve the desired Mach numbers. The cylinder wall temperature is set to 300 K, 500 K, and 1000 K for cases **M3**, **M6**, and **M12** respectively. The DSMC solver assumes diffuse reflection and full thermal accommodation at the cylinder wall. The same mesh is used for all NS, DSMC, and MPC simulations of all cases. The mesh is structured and consists of 600 evenly spaced cells along the surface of the cylinder and 300 cells in the radial direction. In the fore-body, the cell size is clustered towards the cylinder surface. For all cases the cell size is verified to be less than the local mean-free-path throughout the domain. This constraint is a requirement of the DSMC method and is more than sufficient for an accurate NS simulation. The reference particle weight is set to obtain at least 20 particles per cell in the wake region which results in approximately 50 particles per cell, on average, in the fore-body flow. No particle weighting, nearest-neighbor collision routine, or sub-cell sampling is used. Constant DSMC time-steps of 5×10^{-8} s are used for both the **M3** and **M6** cases, while a time-step of 2×10^{-8} s is used for case **M12**. These time-steps are less than one-half of the shortest mean-free-time anywhere in each simulation.

B. Continuum Breakdown and Interface Location

Ultimately, the accuracy of a hybrid particle-continuum method relies on the proper positioning of the DSMC-NS interfaces. The interface must lie in near-equilibrium regions where solution of the NS equations will introduce minimal or no error. Typically, particle and continuum regions are determined by applying a continuum breakdown parameter to the flow field. The MPC method presented in this article uses the gradient-length Knudsen number

$$Kn_{GL-Q} = \frac{\lambda}{Q_{local}}|\nabla Q| \quad , \tag{2}$$

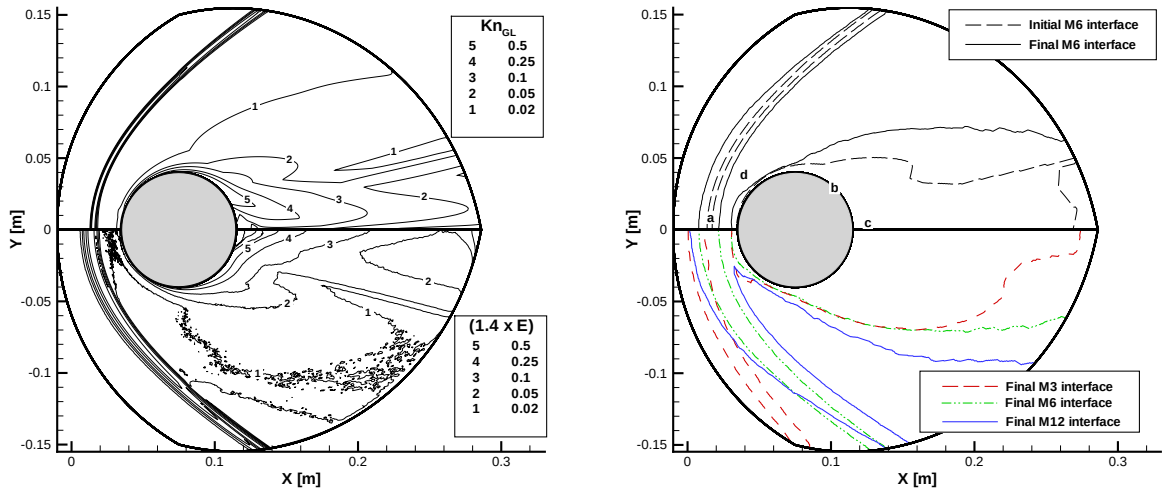

(a) Continuum breakdown.

(b) DSMC-NS interface locations.

Figure 1. Continuum breakdown and interface locations.

where Q represents local flow quantities such as density (ρ), temperature (T), or velocity magnitude ($|V|$), λ is the local mean-free-path, and the gradient is taken in the direction of the maximum gradient. In low speed regions of the flow, it is useful to normalize the velocity gradient by the local speed of sound, a, which can be implemented by setting $Q_{local} = \max(\ |V|,\ a\ )$. The final value used to quantify the degree of local continuum breakdown is then taken as the maximum for all flow quantities,

$$Kn_{GL} = \max(Kn_{GL-\rho}, Kn_{GL-T}, Kn_{GL-|V|}) \quad . \tag{3}$$

It has been shown for flows representative of hypersonic re-entry problems[21] and for 1D normal shock waves,[16] that in regions of the flow field where $Kn_{GL} < 0.05$, the discrepancy between a NS and DSMC solution is less than 5%. Thus, these regions could be solved using a NS solver with little error. The MPC method begins with a NS solution and Fig. 1(a) (top) plots the value of Kn_{GL} from Eq. 3 applied to this initial NS solution for the **M6** case. Figure 1(a) (bottom) also plots the error in this NS solution compared with a full DSMC solution. Specifically, the error E is calculated from

$$E = \max\left|\frac{Q_{NS} - Q_{DSMC}}{Q_{DSMC}}\right| \quad \text{where} \quad Q = \rho,\ T,\ \text{or}\ |V| \ , \tag{4}$$

and the contours in Fig. 1(a) (bottom) actually correspond to values of $1.4 \times E$. Since the contours depict a maximum of several quantities, any apparent discontinuities in Fig. 1(a) are regions where a new quantity has become dominant. As expected, the breakdown parameter is highest in the shock, fore-body boundary layer, and in the near-wake. Regions where Kn_{GL} is large are seen to correspond very well with regions of high error, E. In the near-wake region the error is seen to range from 10-40%. The dominant error in this region is determined to be the velocity magnitude which would likely improve with the use of slip boundary conditions in the NS solver. Quantitatively, Fig. 1(a) reveals that the breakdown parameter predicts the *magnitude* of this error quite well. More specifically, it uniformly over-predicts the error; that is, the contours of Kn_{GL} match quite closely the contours of $1.4 \times E$. Similar agreement is found for cases **M3** and **M12**. These results lend further support to previous recommendations[16,21] of setting breakdown cutoff at $Kn_{GL} = 0.05$. Thus any cell in which the value of $Kn_{GL} > 0.05$ is set as a particle (DSMC) cell and the remaining cells are set as continuum (NS) cells. The initial and final interface locations for this case (**M6**) are shown in the top portion of Fig. 1(b). The initial interface corresponds to contour level 2 in the top of Fig. 1(a) after a simple smoothing algorithm has been applied. The letters **a** through **d** denote regions of interest for later reference. The bottom portion of Fig. 1(b) shows the final interface locations for all three cases presented in this article. Clearly, the higher the flow speed, the larger the non-equilibrium particle region. Note how the particle region ends before the domain exit for case **M3** and how the shock and boundary-layer particle regions merge for the **M12** case.

The continuum breakdown parameter defined in Eq. 3 does not account for thermal non-equilibrium and as a result is unable to position the post-shock interface correctly. As suggested in Ref. 16, this article adds a condition of thermal

equilibrium to the breakdown parameter which now becomes

$$Kn_{GL} = \max\left(Kn_{GL-\rho}, Kn_{GL-T}, Kn_{GL-|V|},\ 5\times\frac{T_{TRA}-T_{ROT}}{T_{ROT}}\right) \quad . \tag{5}$$

In continuum (NS) regions, $T_{TRA} = T_{ROT} = T$, however in particle regions these temperatures may not be equal. Only the very strong thermal non-equilibrium in the shock wave needs attention. This is a compression region in which $T_{ROT} < T_{TRA}$, whereas the remainder of the flow field is in expansion non-equilibrium with $T_{ROT} > T_{TRA}$. In order to focus only on the shock region, the temperature difference in Eq. 5 is calculated without absolute value signs. Thus, in regions where $T_{TRA} > T_{ROT}$ by more than 1%, the breakdown parameter is given a value, $Kn_{GL} > 0.05$. The continuum breakdown paramter expressed by Eq. 5 is used in all cases presented in this article.

C. Information Transfer

The modular implementation of the MPC method allows both DSMC and NS solvers to load and store the same mesh in their own separate data structures. This involves duplication of the mesh geometry but allows for both solvers to operate on their own data structure without modification. Each cell of one mesh is simply linked to the corresponding cell in the other mesh and can easily access its information. Cells labelled as particle cells are simply not used in the NS mesh, and likewise those labelled as continuum cells will contain no particles in the DSMC mesh. This implementation is depicted in Fig. 2 where the cells with dotted lines are stored in memory, but are not used. After application of the breakdown parameter (Kn_{GL}), the particle region is immediately extended by a few extra cells into the continuum domain to create an overlap region. The need for this overlap region will be discussed shortly. Next, one row of NS boundary cells and two rows of DSMC boundary cells are initialized as seen in Fig. 2. Now that all regions of NS and DSMC cells, including boundary cells, have been defined, the regions must be coupled by transferring information across the interface. This is handled through the standard boundary procedures already used by both solvers.

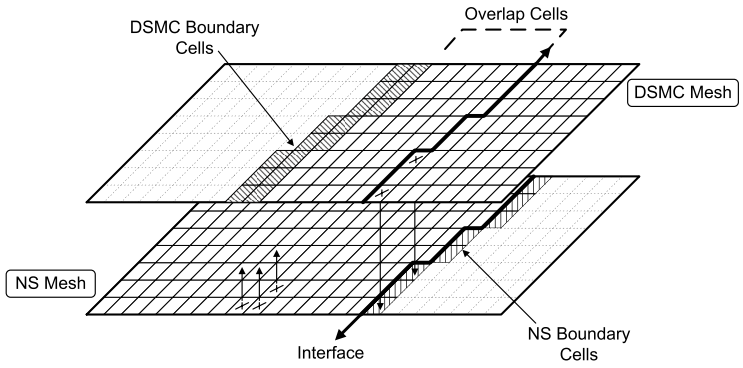

Figure 2. State-based coupling.

The DSMC boundary cells are continually filled with particles consistent with the flow properties in the corresponding NS cell. For each time-step, all simulation particles in the DSMC boundary cells are first deleted and then re-generated based on current NS information. The number of new particles is determined directly from the NS cell density and the particles are randomly distributed within the DSMC boundary cell volume. The velocities of these newly generated particles are sampled from a Chapman-Enskog distribution[22] based on the local macroscopic state and gradients, known from the NS solver. The boundary cells then become an extension of the DSMC domain for one standard DSMC cycle.

As particles in the DSMC domain interact and their distributions evolve in time, the MPC method also tracks the macroscopic variation in each DSMC cell. In order to provide these averaged properties with minimal statistical scatter, a mixture of spatial and temporal averaging is used. Specifically, this study uses the sub-relaxation technique proposed by Sun and Boyd[23] which includes cumulative history using a relaxation factor. This average also allows for "old history" to be removed occasionally in order to follow the true time variation without significant lag. During each time step (j), macroscopic properties (Q_j) are determined simply by averaging over all particles within a cell. Even in high speed flows, these properties (such as ρ, u, v, and T) exhibit significant statistical scatter.[16] With 20-50 particles

per cell, scatter is typically over 20%, and can be as high as 100%. In order to reduce this scatter, the sub-relaxation formula for the *temporal* average of these macroscopic properties ($\overline{Q_j}$) is calculated in each cell as

$$\overline{Q_j} = (1-\theta)\overline{Q_{j-1}} + \theta Q_j \quad . \tag{6}$$

Here, θ is the small weight given to each new cell-averaged property and $(1-\theta)$ is a larger weight applied to the previous history. The correction, which removes "old history" is given by

$$\overline{Q_j}' = \overline{Q_j} + \frac{(1-\theta)^{j-i}}{1-(1-\theta)^{j-i}} \left(\overline{Q_j} - \overline{Q_i}' \right) \quad , \tag{7}$$

where j is the current time-step, i is the previous time-step at which a correction was made, and $\overline{Q_i}'$ is the temporal average recorded at this previous time-step i. As detailed in Ref. 23, Eqn. 7 effectively removes the history before time-step i. In order to maintain stability, this correction is performed only when the coefficient of this correction is between zero and one. This condition is approximately satisfied when $j = \frac{1}{\theta} + i$. Thus, the sub-relaxation technique provides macroscopic quantities in each DSMC cell at each time-step. At the desired time, these averaged DSMC properties can then be used as boundary conditions for the NS solver. The final aspect of a hybrid method is the numerical cycle which determines *when* to transfer information between particle and continuum regions.

D. MPC Numerical Cycle

The MPC numerical cycle loosely couples the two solvers to first position all interfaces in near-continuum regions, and then proceed to both sample the DSMC and converge the NS regions. The cycle consists of the following general steps:

1. Using Kn_{GL}, setup the initial DSMC and NS domains based on an initial NS solution. Generate particles throughout the entire DSMC domain.

2. Allow DSMC regions to evolve with the current boundary conditions, while adaptively repositioning the interfaces (utilizing the overlap region) without using the NS solver at all.

3. After the DSMC solution and interfaces stop changing, use the current DSMC solution to set the NS boundary conditions. Significantly converge the NS region.

   IF the new NS solution changes the state in any DSMC boundary cell $\longrightarrow$ return to 2.

   ELSE , if the new NS solution does not changes the state in any DSMC boundary cell $\longrightarrow$ continue to 4.

4. Since the NS region is converged *and* the DSMC solution is no longer changing, the interfaces will no longer change and steady-state has been reached. Lock the interfaces and cycle both the DSMC and NS solvers (coupling occasionally) until the DSMC scatter and NS residual fall below threshold values.

Evolution of the MPC temperature profile along the stagnation streamline is shown in Fig. 3 for case **M6**. At the beginning of a hybrid simulation, the breakdown parameter is applied to a NS solution. As depicted in Fig. 3(a), this results in initial interfaces enclosing the thin NS shock profile and an overlap region is extended 10 cells further on either side. Initially, this DSMC region (including the overlap region) is filled with particles consistent with the NS solution. Then, as the DSMC solver iterates, the particle distributions evolve significantly towards the correct non-equilibrium solution. For example, at the pre-shock interface in Fig. 3(a), the temperature is seen to rise from its initial value of 217 K to a value of over 1000 K. Figure 3(b) shows how the sub-relaxation technique follows this change where the data corresponding to $\theta = 1.0$ represents only the spatial average for temperature, which exhibits significant statistical scatter. Using temporal averaging, the sub-relaxation average with $\theta = 0.002$ is seen to eliminate the scatter while introducing a time-lag in the temperature variation. However, since the MPC method is designed for steady-state flows, this time-lag is acceptable whereas high statistical scatter is not. The MPC profile inside the DSMC and overlap region (the solid line in Fig. 3(a)) is the result of using the sub-relaxation technique. As the particle region evolves, the breakdown parameter is occasionally applied to this MPC profile. As seen in Fig. 3(a), since the overlap region now contains significant flow gradients, Kn_{GL} may be larger than the 0.05 cutoff value. If so, the interfaces will widen and new overlap regions will be extended by a further 10 cells. In this way, the interfaces adapt based on DSMC data only. When the DSMC solution stops changing and interfaces are ensured to be in near-equilibrium regions, the new DSMC solution is used to set the NS boundary conditions. The NS region is then converged significantly

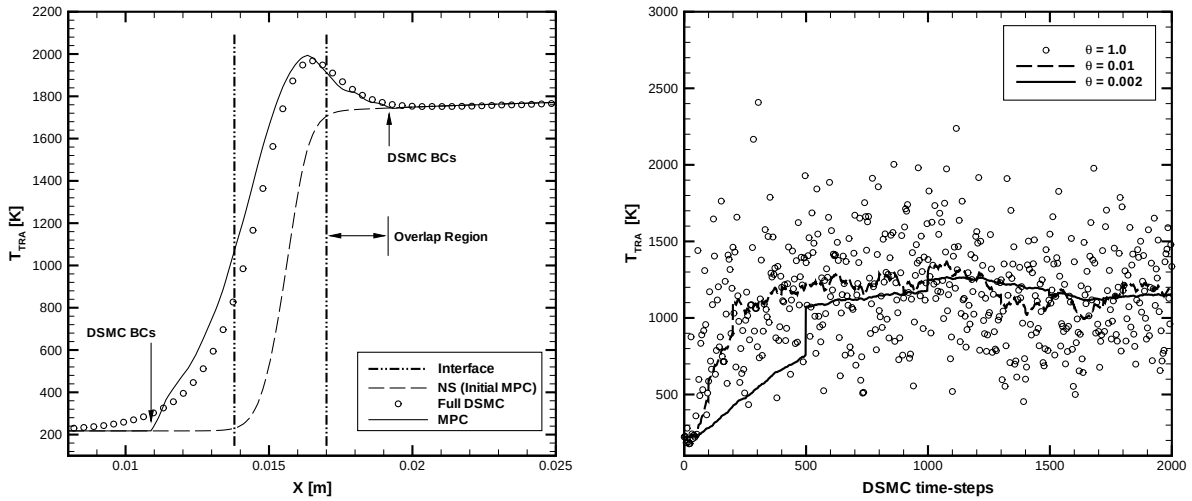

(a) Evolution of MPC temperature along a stagnation streamline.

(b) Sub-relaxation average.

Figure 3. MPC coupling procedure.

using an implicit method with a CFL number of 5.0. When focusing on steady-state flows, this time-scale decoupling allows for much larger NS time-steps and thus requires relatively few NS iterations compared to DSMC. If the new NS solution has not altered the state in any of the DSMC boundary cells then interface locations are locked. At this point steady-state has been reached and the sub-relaxation average is replaced with cumulative sampling which enables the scatter to be completely removed. Both solvers are then loosely coupled across these fixed interfaces. Specifically, every 5000 DSMC sampling time-steps information is transferred to the NS region which is then converged for 100 implicit time-steps. This cycle repeats until both the DSMC scatter and NS residual fall below threshold values.

III. Numerical Investigation of Non-Equilibrium Regions

A. Velocity distribution functions

In order to investigate the degree of non-equilibrium in hypersonic blunt body flow fields, it is instructive to look at the local velocity distribution function (vdf). The MPC solver uses DSMC in non-equilibrium regions and the NS equations in near-equilibrium regions where the local vdf should be a Chapman-Enskog distribution. Thus, the MPC code has all the information required to generate the physically correct vdf at every location in the flow. The local vdfs for four regions of interest (labelled **a** through **d** in Fig. 1(b)), are generated using full DSMC, full NS, and MPC simulations for case **M6** and shown in Fig. 4. The first observation from all vdfs plotted in Fig. 4 is that the MPC particles do indeed have the same velocity distribution as particles within a full DSMC simulation. The most severe non-equilibrium region is in the shock center along the stagnation streamline (region **a**), shown in Fig. 4(a). In order to adjust for the different shock positions between DSMC and NS solutions, the shock center is taken as the point where $T_{TRA} = 0.5(T_{TRA\ post} + T_{TRA\ pre})$ for DSMC and MPC, and where $T = 0.5(T_{post} + T_{pre})$ in the NS solution. The dotted lines shown in Fig. 4 are Chapman-Enskog distributions generated[22] using the local NS state and gradients. In Fig. 4(a), the vdf in the *x*-direction shows a peak of fast moving particles, but also a significant number of post-shock particles which have travelled upstream through the thin shock and maintained their low speed. The Chapman-Enskog distribution effectively assumes more collisions and thus the fast moving peak is lowered and the slow moving region of the vdf is raised. Certainly the NS equations do not contain the information needed to describe the vdf in either the *x* or *y* direction inside the shock. Another region of the flow which is highly non-equilibrium is region **b**, located 135^o around the cylinder surface. The local vdfs are plotted in Fig. 4(b) where the Chapman-Enskog vdfs are centered around zero velocity due to the no-slip condition in the NS solver. In addition to significant velocity slip, evident in the DSMC and MPC vdfs, Fig. 4(b) reveals that the vdf in the *y* direction is quite far from having an equilibrium shape. The local vdf in a cell 2 *cm* directly behind the cylinder (region **c**) is plotted in Fig. 4(c). Here the DSMC and MPC vdfs appear quite similar to the Chapman-Enskog distribution from the NS solution, only they are slightly

wider. It will be shown in the next section that this width does indeed correspond to a higher temperature in this region. Finally, for region **d**, which lies downstream of the shock but away from the surface, Fig. 4(d) shows that the DSMC distribution is indeed a Chapman-Enskog distribution. In addition, this is a continuum region of the mesh where the MPC method solves the NS equations. Figure 4(d) demonstrates how the NS equations are sufficient to represent the local vdf in this region. It should be noted that because of the large velocity scales in these vdf plots, it is difficult to determine the degree to which small variations in a vdf translate into noticeable macroscopic effects. For this reason the flow field and surface properties are now investigated.

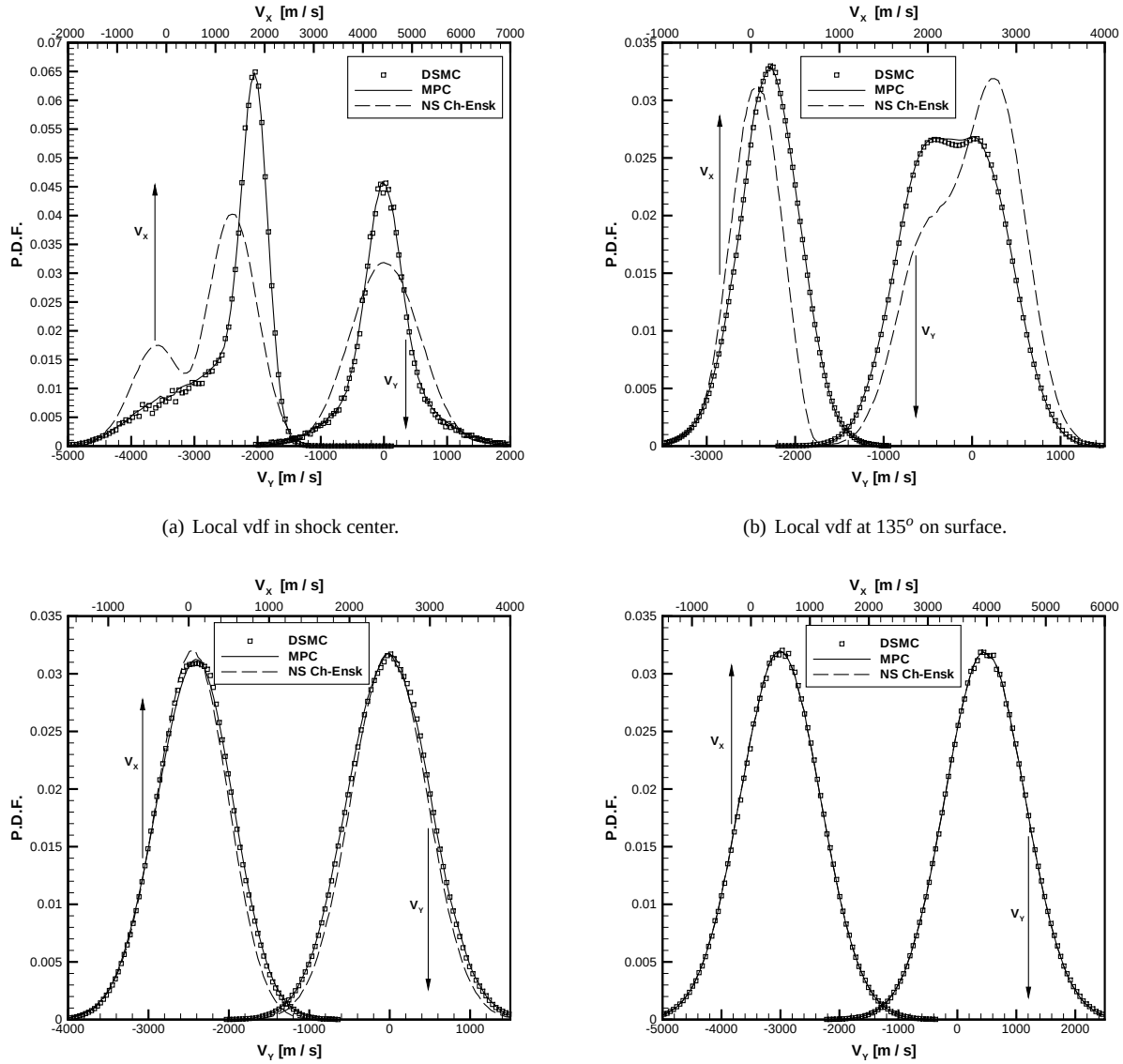

(a) Local vdf in shock center.

(b) Local vdf at 135^o on surface.

(c) Local vdf in near-wake region.

(d) Local vdf in post-shock continuum region.

Figure 4. Local velocity distribution functions for case M6.

B. Fore-body and near-wake flow field

The purpose of the MPC method is ultimately to reproduce the flow field and surface property results of a full DSMC simulation in less time. It is important to re-iterate the fact that all MPC results plotted are composed of a NS solution in continuum regions and a sampled DSMC solution in particle regions. The sub-relaxation average is only used while adapting the interfaces and DSMC sampling does not begin until after the interfaces are fixed. The T_{TRA} fields calculated by full DSMC, full NS, and MPC solvers are compared in Fig. 5 for the **M12** case. The DSMC shock wave

is significantly thicker and begins further upstream compared with the NS shock profile. In addition, the translational temperature overshoot is clearly visible in the DSMC solution. The wake region also shows that the temperature predicted by DSMC is approximately $10-15\%$ higher than that predicted by the NS solver. Qualitatively, very similar results are obtained for cases **M3** and **M6**. Figure 5 also shows how the MPC method successfully reproduces a full DSMC solution with little error. In fact the largest error at any location in the flow, for any flow variable, (see Eq. 4, replacing Q_{NS} with Q_{MPC}) is determined to be less than 3.0%, 2.5%, and 1.5% for cases **M12**, **M6**, and **M3** respectively. Moreover, the largest error is in the T_{TRA} field which is maximum in MPC-continuum regions where the NS equations cannot predict thermal non-equilibrium. This may be quite acceptable since conditions in the boundary layer and near-wake regions are of most importance. The MPC solver correctly models these regions as particle regions in which DSMC results are reproduced almost exactly.

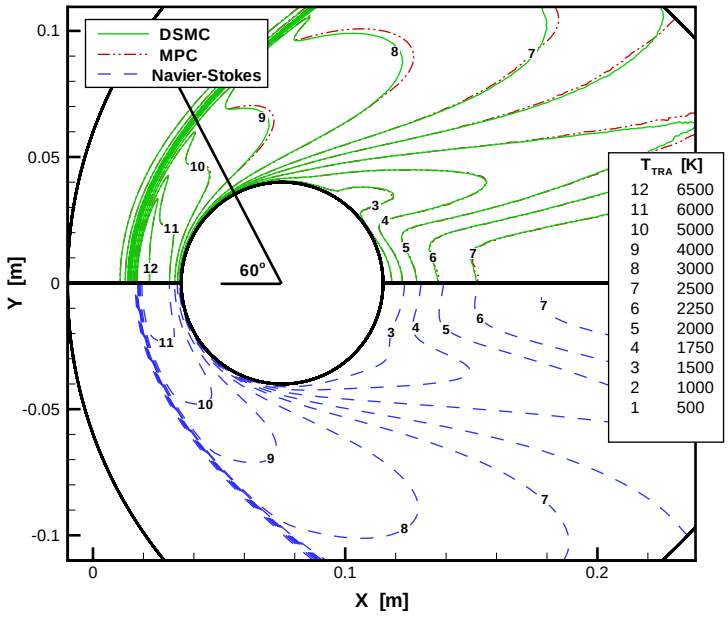

Figure 5. Mach 12 translational temperature field.

A more detailed comparison is shown in Fig. 6(a) where both the translational and rotational temperature profiles are plotted for each solver along the 60^o line shown in Fig. 5. In this region, the flow begins to expand immediately after passing through the shock wave. Since rotational energy requires more collisions to "equilibriate" than the translational energy, it remains frozen at a higher rotational temperature in this expanding region of the flow. Focusing only on the DSMC results, this behavior can be seen in Fig. 6(a). Moving focus to the MPC results, Fig. 6(a) shows how the MPC method predicts the correct profiles for both T_{TRA} and T_{ROT} in both the shock and boundary layer particle regions. However, in the MPC-continuum region between these interfaces, the NS equations are solved which use a single temperature combining both translational and rotational modes. As expected, the MPC temperature profile in this region lies between the T_{TRA} and T_{ROT} profiles predicted by DSMC. Finally, focusing on the full NS solution in Fig. 6(a), it is important to notice that at the interface just after the shock, the MPC temperature is not equal to the initial NS temperature. This means that the MPC cycle has succeeded in providing more accurate boundary conditions to the MPC-continuum region. These conditions were set (or transferred) using the MPC-particle region and result in shifting the MPC-continuum profile to a lower, more accurate translational temperature. However, in this case, the shift is not significant and begs the question; if the post-shock state for both DSMC and NS solutions is virtually the same, is it even necessary to accurately predict the shock interior? In order to answer this question, two additional MPC simulations are tested. The first, denoted **M12a**, only models the boundary layer and wake region as particle regions. That is, the shock is simulated as a continuum region where the NS equations are solved. This approach is similar to the "zonally decoupled" solutions discussed earlier.[3–5] However, the MPC method adapts the interface locations and restricts particle regions only to that portion of the flow field where large non-equilibrium effects are felt. For the **M12** case these regions include the fore-body boundary layer and only a portion of the wake. The second

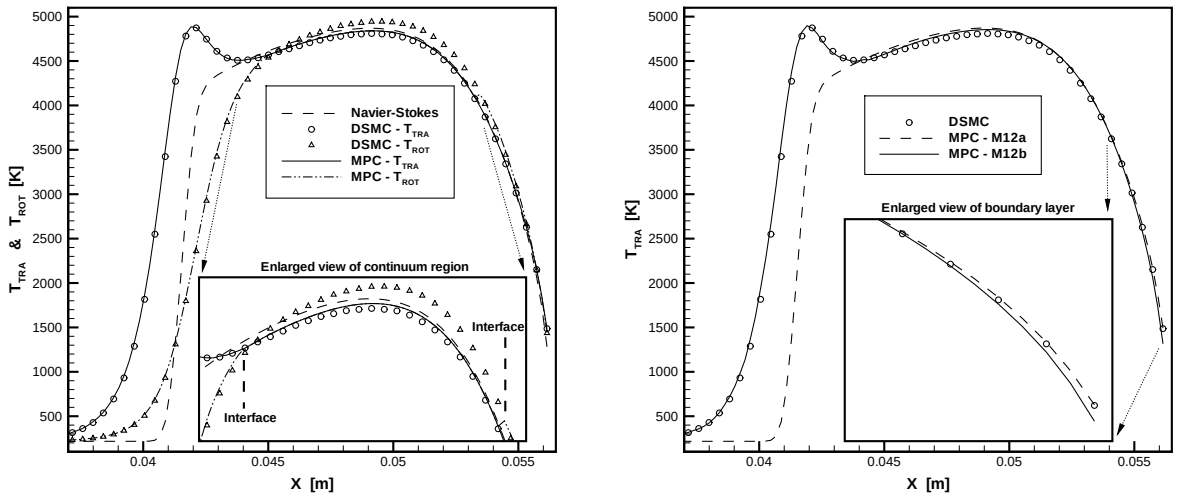

(a) Thermal non-equilibrium effects.

(b) Effect of accurately solving the shock interior.

Figure 6. Fore-body temperature profiles along a 60^o cut.

simulation, denoted **M12b**, models only the shock with a particle region and solves the NS equations everywhere else. Both cases use the exact same flow conditions, mesh, and numerical parameters as the **M12** case and only differ in the final MPC interface locations. The translational temperature profiles along the same 60^o cut are shown in Fig. 6(b). Although case **M12a** does not predict the correct shock profile, since it models the non-equilibrium boundary layer as a particle region, it agrees well with DSMC results near the surface. Conversely, although case **M12b** predicts the correct shock profile, since the post-shock state is only slightly different, the rest of the solution agrees very well with a full NS simulation. Near the cylinder surface, a continuum solution (such as case **M12b**) predicts steeper gradients which may influence the predicted heat transfer and momentum transfer to the spacecraft. Thus, based on the fore-body flow field, modelling the shock wave as a particle region may not be necessary. This will be verified in the next section by examining the predicted surface properties over the entire cylinder.

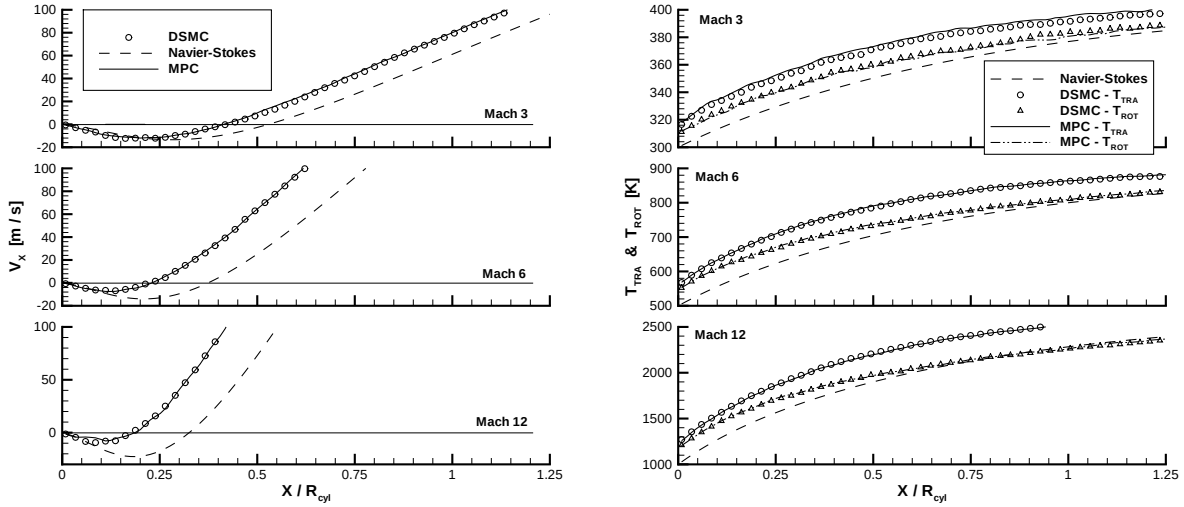

(a) Wake closure.

(b) Near-wake temperature profile.

Figure 7. Non-equilibrium effects in the near-wake region.

Non-equilibrium effects in the near-wake region are portrayed in Fig. 7. The *x*-velocity profiles along the symmetry

axis, directly in the wake of the cylinder, are plotted in Fig. 7(a) for the **M3**, **M6**, and **M12** cases. Here, the location at which the x-velocity becomes positive, indicates the location of "wake closure". For each free-stream Mach number, DSMC simulations predict wake closure to occur closer to the cylinder than predicted by a full NS simulation. In addition, higher Mach number flow, associated with larger non-equilibrium effects, is observed to result in a smaller wake closure length. Both of these results agree qualitatively with those presented in Ref. 3 which compared DSMC and NS results for a slightly more complicated geometry at higher flow speeds. The temperature profiles in the near-wake region are plotted in Fig. 7(b) for all three cases. The wake flow is seen to be slightly out of thermal equilibrium (which the NS equations are not able to predict). In addition, as seen previously in Fig. 5 the translational temperature predicted by DSMC is higher than that predicted by a NS solution. Although not shown, the density in this region is correspondingly lower for DSMC, while the pressure predicted by both NS and DSMC remain similar. Finally, for each of the near-wake results plotted in Fig. 7, the MPC method is seen to reproduce the DSMC profiles with little error. Although not shown, case **M12a** is verified to reproduce DSMC wake results while case **M12b** reproduces full NS results.

C. Surface properties

This article presents for the first time in the literature, a detailed analysis of the surface properties predicted by a hybrid DSMC-NS solver. Figure 8 plots the coefficients of heat transfer (C_q) and shear-stress ($C_{\tau_{||}}$) around the cylinder surface for cases **M3**, **M6**, **M12**, and **M12a**. The coefficients are defined as

$$C_q = \frac{q}{\frac{1}{2}\rho_\infty u_\infty^3} \qquad \text{and} \qquad C_{\tau_{||}} = \frac{\tau_{||}}{\frac{1}{2}\rho_\infty u_\infty^2} \ , \tag{8}$$

where q is the heat transferred to the cylinder per unit time per unit area and $\tau_{||}$ is the tangential momentum per unit time per unit area transferred to the cylinder at each point on the surface. In a NS simulation, both q and τ are determined using gradients of macroscopic flow properties (temperature and velocity). In a DSMC simulation, q and τ are determined by averaging changes in the kinetic energy and momentum of individual particles as they collide with the the surface. In all MPC simulations, as depicted earlier in Fig. 1(b), a particle region envelopes the entire cylinder surface. Thus heat and momentum transfer in the MPC simulations are determined in the same way as in a full DSMC simulation. It is evident that for each flow Mach number in Figs. 8(a)-8(c), the heat and momentum transfer predicted by DSMC are less than those predicted by the NS solver around the entire cylinder. This is due in part to velocity and temperature slip at the surface which is not modelled in the NS simulations but is a natural result of the DSMC simulations. However, it is also due to the fact that in assuming more collisionality, the NS equations predict more rapid flow changes (steeper gradients) which correspond to higher rates of heat and momentum flux. The discrepancy in the peak heating rate is seen to be 4.4%, 10.0%, and 7.5% for cases **M3**, **M6**, and **M12** respectively. The largest difference between DSMC and NS is in the wake of the cylinder where the shear-stress is significantly less according to DSMC. These results are qualitatively and quantitatively similar to those presented in Ref. 24 for simulations of Mach 10 flow of argon around a cylinder. However, as shown in that study, the coefficient of pressure (C_p) predicted by both NS and DSMC is virtually the same. Since the majority of drag on the cylinder is due to pressure drag, despite differences in shear-stress, the total drag on the cylinder remains the same for both NS and DSMC. Again, Figs. 8(a)-8(c) demonstrate how the MPC method successfully reproduces DSMC results. What is also evident in Fig. 8(c) is that when the shock is not modelled using a particle region (case **M12a**), the surface properties are still accurately predicted. In the fore-body, up to an angle of approximately 30^o, the heat transfer is seen to be slightly higher, but elsewhere the results are identical. Also, as expected, the **M12b** case, which captures the shock accurately with a particle region but uses the NS equations everywhere else, predicts surface properties consistent with a full NS solver. Although barely discernable, compared with the full NS solution, case **M12b** predicts a slightly lower heat transfer in the fore-body due to the slightly different post-shock state.

D. Computational Efficiency of the MPC Method

In limiting particle domains only to regions of highly non-equilibrium flow, the MPC method uses far fewer particles than a full DSMC simulation and as a result saves significant computational time. The efficiency of the MPC method is plotted in Fig. 8(d) for each of the four cases which successfully reproduce DSMC results. Here the dotted line represents the ideal speedup factor which is simply equal to the ratio of particles in a full DSMC simulation to that required by the MPC method. The time required by a DSMC solver scales linearly with the number of simulated particles. Thus if the MPC method was able to use 4 times fewer particles and all hybrid operations were free, it could reach the answer 4 times faster at best. In order to compare the computational time required for DSMC and

MPC solutions, simulations are divided into two stages; the time required to reach steady-state and the sampling time. For a DSMC simulation, steady-state is reached when the total number of particles stops increasing and becomes constant. For the MPC simulation, reaching steady-state involves the time required for the initial NS solution plus the time required for the MPC interfaces to adapt to their final positions and be locked in place. A fair comparison then

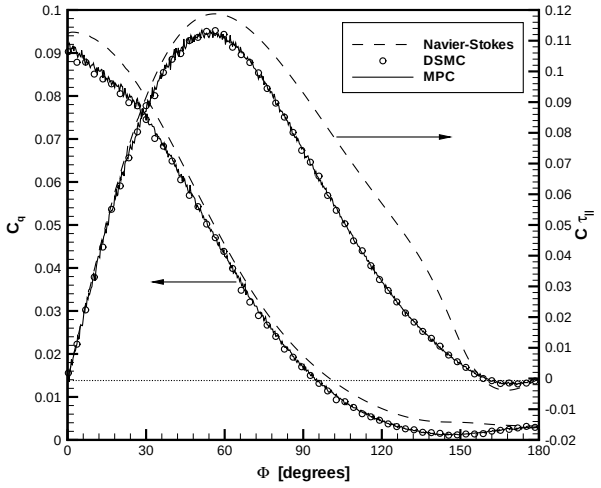

(a) Mach 3 surface properties.

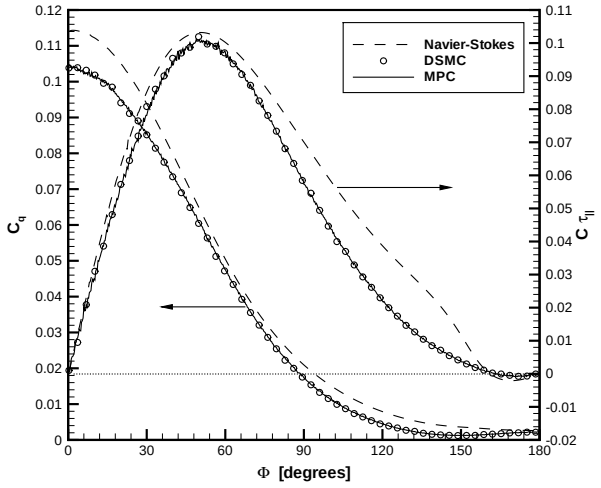

(b) Mach 6 surface properties.

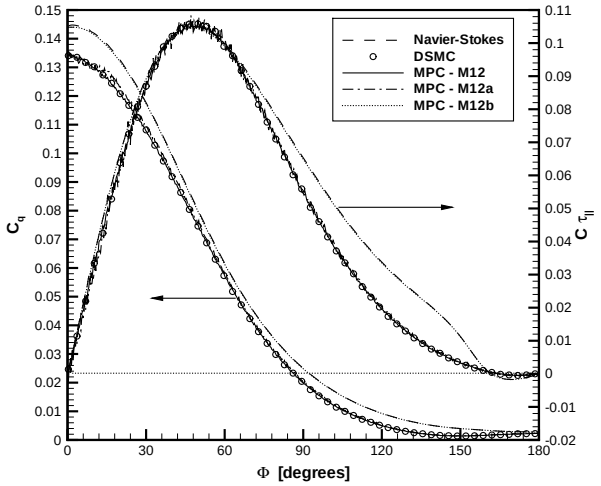

(c) Mach 12 surface properties.

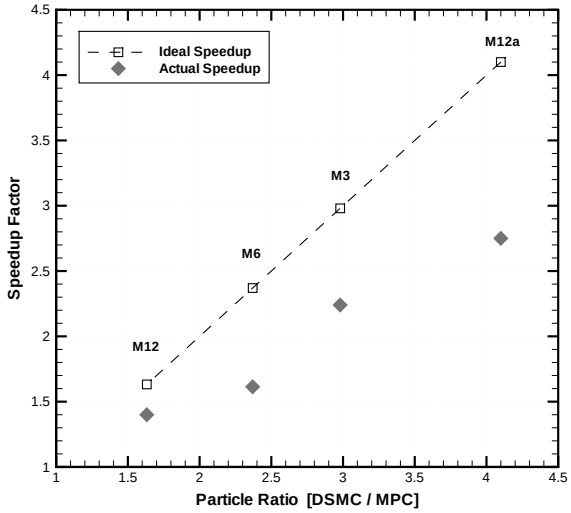

(d) MPC computational efficiency.

Figure 8. Surface properties and MPC efficiency.

requires both DSMC and MPC simulations to be sampled for the same number of DSMC time steps. Sampling the MPC solution involves fewer particles but also requires coupling to the NS solver and NS iterations of the continuum regions. The total simulation time for both solvers is then the sum of these two stages. The actual speedup factors for each case are shown in Fig. 8(d) as the solid symbols. They are seen to be proportional to the number of particles saved by the MPC method (the particle ratio) which is proportional to the amount of the flow field which can be assumed as near-equilibrium flow. The **M12**, **M6**, and **M3** cases are seen to run 1.4, 1.6, and 2.2 times faster respectively. Furthermore, by not modelling the shock wave as a particle region in case **M12a**, a large number of particles are eliminated since the shock is a dense region of the flow. The result is a speedup of 2.8 times where, as previously shown, aside from the internal shock structure the MPC results accurately reproduce a full DSMC simulation. It should be noted that the initial NS solution accounts for roughly 50% of the difference between actual and ideal

speedups for each case shown in Fig. 8(d). This is due to the fact that the NS solver currently uses the same mesh as DSMC, which is refined to the mean-free-path. For the cases discussed in this article, a mesh which meets DSMC requirements contains roughly 10 times as many cells as a mesh designed to meet NS requirements. In addition, NS iterations on this fine mesh during the MPC coupling cycle also contribute to the overhead. Thus, by allowing the NS solver to operate on a coarser mesh, a large portion of the MPC overhead could be eliminated. Finally, the third major source of overhead involves the averaging calculations required to track the sub-relaxation average in each DSMC cell at each time-step. Depending on acceleration techniques used in individual DSMC and NS solvers, absolute simulations times may certainly vary. However, since the MPC method couples existing solvers (un-modified), the speedup factors determined here should apply in general.

IV. Conclusions and Future Direction

In conclusion, a modular particle-continuum (MPC) numerical scheme was able to successfully reproduce DSMC results for simple hypersonic blunt body flows in less time. By focusing on steady-state flows, temporal averaging using a sub-relaxation technique is able to effectively control statistical scatter in particle regions. In addition, state-based coupling utilizes the existing boundary procedures of both DSMC and NS solvers. This enables both solvers to be used virtually un-modified as modules in the MPC code. In regions of continuum breakdown, the gradient-length Knudsen number is shown to provide a reasonable prediction for the magnitude of error in a NS solution. MPC simulations show that in regions of the flow field where this parameter is less than 0.05, solution of the NS equations provide accurate results. For hybrid simulations involving strong shock waves an additional condition of thermal equilibrium is required in the definition of continuum breakdown. The MPC method is shown to accurately reproduce macroscopic flow fields, local velocity distributions, and surface properties of steady-state DSMC simulations. Analysis of local velocity distributions reveal that large regions of the flow field, such as between the shock and boundary layer, contain equilibrium particle distributions and can thus be modelled accurately by the NS equations. At the same time, the velocity distributions inside the shock wave and in the near-wake region are found to deviate significantly from near-equilibrium (Chapman-Enskog) distributions. As a result, NS solutions become inaccurate in these regions. For 2D flow of N_2 over a cylinder at various Mach numbers where the global Knudsen number is 0.01, NS simulations significantly over-predict the local shear-stress. However, this has a negligible effect on the total drag since the predicted pressures from DSMC and NS are similar. In addition, the NS simulations are found to over-predict the peak heating rate by 5-10% while predicting slower wake closure and 10-15% lower temperatures in the immediate wake region. The MPC code is able to accurately reproduce these DSMC results where the maximum error in any variable, at any location, is 3%. This maximum error is in temperature and is found away from the cylinder surface in MPC-continuum regions where the NS equations cannot predict thermal non-equilibrium. This error is acceptable since the boundary layer and near-wake regions are of more importance for the prediction of surface properties. The MPC method accurately models these regions using DSMC and as a result the error in these regions and in the surface properties is negligible. The MPC method achieves this accuracy with speedup factors of 1.4, 1.6, and 2.2 for free-stream Mach numbers of 12, 6, and 3 respectively. The computational time saved by the MPC method is directly proportional to the fraction of the flow field which is in near-equilibrium. It is found that particle simulation of the shock interior is not necessary for accurate prediction of surface properties, however particle simulation of the boundary layer and near-wake region is. When an MPC simulation of Mach 12 flow is repeated without particle simulation of the shock wave, the speedup factor rises to 2.8 with no noticeable loss of accuracy.

Currently, both DSMC and NS modules of the MPC code operate on the same computational mesh, which is refined to meet DSMC specifications. Without any loss of accuracy, NS regions could use a much coarser mesh. This could significantly reduce the MPC overhead since the initial NS solution and NS updates within the MPC cycle would require much less time. Additionally, the MPC code must be upgraded with parallel computing capabilities. This is necessary to simulate the higher speed, lower Knudsen number flows of practical interest, where DSMC becomes very computationally intensive. Such flows may be almost entirely within the continuum regime but still exhibit important non-equilibrium effects in near-wake regions. The ratio of particles saved and thus the speedup potential for the MPC method should be significantly higher for such flows. Finally, in order to simulate practical re-entry flows, multi-species capability, vibrational energy exchange, and chemistry must be included in the MPC code. These physical models already exist in both the DSMC and NS solvers. It is the control of statistical scatter and information transfer associated with these processes which requires additional research.

Acknowledgments

This work is sponsored by the Space Vehicle Transportation Institute, under NASA grant NCC3-989 with joint sponsorship from the Department of Defense and from the Air Force Office of Scientific Research grant FA9550-05-1-0115. This work is also supported by the Francois-Xavier Bagnoud Foundation and the University of Michigan, Horace H. Rackham School of Graduate Studies.

References

[1]Bird, G. A., *Molecular Gas Dynamics and the Direct Simulation of Gas Flows*, Oxford University Press, New York, 1994.

[2]Moss, J. N. and Price, J. M., "Survey of Blunt Body Flows Including Wakes at Hypersonic Low-Density Conditions," *Journal of Thermophysics and Heat Transfer*, Vol. 11, No. 3, 1997, pp. 321–329.

[3]Wilmoth, R. G., Mitcheltree, R. A., Moss, J. N., and Dogra, V. K., "Zonally Decoupled Direct Simulation Monte Carlo Solutions of Hypersonic Blunt-Body Wake Flows," *Journal of Spacecraft and Rockets*, Vol. 31, No. 6, 1994, pp. 971–979.

[4]Glass, C. E. and Gnoffo, P. A., "A 3-D Coupled CFD-DSMC Solution Method With Application to the Mars Sample Return Orbiter," *NASA TM-2000-210322*, July 2000.

[5]Glass, C. E. and Horvath, T. J., "Comparison of a 3-D CFD-DSMC Solution Methodology With a Wind Tunnel Experiment," *NASA TM-2002-211777*, Aug. 2002.

[6]Wijesinghe, H. S. and Hadjiconstantinou, N. G., "A Discussion of Hybrid Atomistic-Continuum Methods for Multiscale Hydrodynamics," *International Journal for Multiscale Computational Engineering*, Vol. 2, 2004.

[7]Hash, D. B. and Hassan, H. A., "Assessment of Schemes for Coupling Monte Carlo and Navier-Stokes Solution Methods," *Journal of Thermophysics and Heat Transfer*, Vol. 10, No. 2, 1996, pp. 242–249.

[8]Hash, D. B. and Hassan, H. A., "A Decoupled DSMC/Navier-Stokes Analysis of a Transitional Flow Experiment," *AIAA Paper 96-0353*, Jan. 1996, presented at the 34th AIAA Aerospace Sciences Meeting and Exhibit, Reno, NV.

[9]Wijesinghe, H. S., Hornung, R. D., Garcia, A. L., and Hadjiconstantinou, N. G., "Three-dimensional Hybrid Continuum-Atomistic Simulations For Multiscale Hydrodynamics," *Journal of Fluids Engineering*, Vol. 126, 2004, pp. 768–777.

[10]Hash, D. B. and Hassan, H. A., "Two-Dimensional Coupling Issues of Hybrid DSMC / Navier-Stokes Solvers," *AIAA Paper 97-2507*, June 1997, presented at the 32nd AIAA Thermophysics Conference, Atlanta, GA.

[11]Roveda, R., Goldstein, D. B., and Varghese, P. L., "Hybrid Euler/Particle Approach for Continuum/Rarefied Flows," *Journal of Spacecraft and Rockets*, Vol. 35, No. 3, 1998, pp. 258–265.

[12]Roveda, R., Goldstein, D. B., and Varghese, P. L., "Hybrid Euler/Direct Simulation Monte Carlo Calculation of Unsteady Slit Flow," *Journal of Spacecraft and Rockets*, Vol. 37, No. 6, 2000, pp. 753–760.

[13]Sun, Q. and Boyd, I. D., "A Direct Simulation Method for Subsonic, Micro-Scale Gas Flows," *Journal of Computational Physics*, Vol. 179, 2002, pp. 400–425.

[14]Wang, W.-L. and Boyd, I. D., "Hybrid DSMC-CFD Simulations of Hypersonic Flow over Sharp and Blunted Bodies," *AIAA Paper 03-3644*, 2003, presented at the 36th AIAA Thermophysics Conference, Orlanda, Fl.

[15]Wang, W.-L. and Boyd, I. D., "A New Energy Flux Model in the DSMC-IP Method for Nonequilibrium Flows," *AIAA Paper 03-3774*, 2003, presented at the 36th AIAA Thermophysics Conference, Orlanda, Fl.

[16]Schwartzentruber, T. E. and Boyd, I. D., "A hybrid particle-continuum method applied to shock waves," *Journal of Computational Physics*, Vol. 215, 2006, pp. 402–416.

[17]Dietrich, S. and Boyd, I. D., "Scalar and Parallel Optimized Implementation of the Direct Simulation Monte Carlo Method," *Journal of Computational Physics*, Vol. 126, 1996, pp. 328–342.

[18]Boyd, I. D., "Analysis of Rotational Nonequilibrium in Standing Shock Waves of Nitrogen," *AIAA Journal*, Vol. 28, No. 11, 1990, pp. 1997–1999.

[19]Scalabrin, L. C. and Boyd, I. D., "Development of an Unstructured Navier-Stokes Solver for Hypersonic Nonequilibrium Aerothermodynamics," *AIAA Paper 05-5203*, 2005, presented at the 38th AIAA Thermophysics Conference, Toronto, Ontario, Canada.

[20]MacCormack, R. W. and Candler, G. V., "The Solution of the Navier-Stokes Equations Using Gauss-Seidel Line Relaxation," *Computers and Fluids*, Vol. 17, 1989, pp. 135–150.

[21]Boyd, I. D., Chen, G., and Candler, G. V., "Predicting Failure of the Continuum Fluid Equations in Transitional Hypersonic Flows," *Physics of Fluids*, Vol. 7, No. 1, 1995, pp. 210–219.

[22]Garcia, A. L. and Alder, B. J., "Generation of the Chapman-Enskog Distribution," *Journal of Computational Physics*, Vol. 140, 1998, pp. 66–70.

[23]Sun, Q. and Boyd, I. D., "Evaluation of Macroscopic Properties in the Direct Simulation Monte Carlo Method," *Journal of Thermophysics and Heat Transfer*, Vol. 19, No. 3, 2005, pp. 329–335.

[24]Lofthouse, A. J., Boyd, I. D., and Wright, M. J., "Effects of Continuum Breakdown on Hypersonic Aerothermodynamics," *AIAA Paper 06-993*, Jan. 2006, presented at the 44th AIAA Aerospace Sciences Meeting and Exhibit, Reno, NV.